Original

Feistauer, E.; Bergmann, L.; dos Santos, J.F.:

Performance of friction stir welded tailor welded blanks in AA5059 and AA6082 alloys for marine applications

In: Key Engineering Materials, Aluminium Constructions: Sustainability, Durability and Structural Advantages (2016) Trans Tech Publications

DOI: 10.4028/www.scientific.net/KEM.710.91

Key Engineering Materials
ISSN: 1662-9795, Vol. 710, pp 91-96
doi:10.4028/www.scientific.net/KEM.710.91

Submitted: 2016-04-16
Revised: 2016-06-02
Accepted: 2016-06-28
Online: 2016-09-23

Performance of Friction Stir Welded Tailor Welded Blanks in AA5059 and AA6082 Alloys for Marine Applications

Eduardo E. Feistauer [1,a*], Luciano Bergmann[1,b] and Jorge F. dos Santos[1,c]

[1] Helmholtz-Zentrum Geesthacht, Institute of Materials Research, Materials Mechanics, Solid-State Joining Processes, Max-Planck-Str. 1, 21502 Geesthacht, Germany.

[a*]eduardo.feistauer@hzg.de, [b]luciano.bergmann@hzg.de, [c]jorge.dos.santos@hzg.de

Keywords: Tailor welded blanks, Friction stir welding, Local and global mechanical properties

Abstract. Tailor welded blank (TWB) concepts in aluminum alloys, welded by friction stir welding (FSW), are an attractive solution to reduce structural weight of structures applied on the transportation sector. In the present work the mechanical performance and microstructural features of dissimilar friction stir welded TWBs were assessed. Welds were produced with alloys of particular interest to the shipbuilding sector (AA6082 and AA5083, with a thickness combination of 6 and 8 mm respectively) and the effect of rotational speed on the weld properties was investigated. A digital image correlation system (DIC) was used to characterize the local strain fields during the quasi-static tensile tests. Microstructure analysis revealed the presence of a remnant oxide line (ROL) at the stir zone. Moreover, the rotational speed directly affected the ROL distribution and consequently the mechanical properties of the welds. The TWB produced with low rotation speed and high force (600 rpm and 20kN) has shown the highest mechanical performance and failed at the thermo-mechanically affected zone of the AA6082 plate. The micromechanisms of fracture were assessed by SEM and revealed a ductile fracture with large amounts of dimples spread out on the fracture surface.

Introduction

The transport sector is being driven by developments, which not only require the fulfilment of severe environmental regulations, but also promote weight reduction, increased productivity and reduction of production costs. Hence, the use of lightweight alloys on the shipbuilding sector has significantly increased over the last few decades, manly as an alternative for manufacturing lightweight fuel-efficient and high-speed crafts [1]. In this context, tailor welded blank (TWB) concepts in aluminum alloys welded by friction stir welding (FSW) are an attractive alternative solution to accomplish these requirements.

TWB consist of adequately tailor material properties, so that it can efficiently fulfil mechanical requirements and, at the same time reduce weight and production costs of formed structures. In order to achieve that, local variation on thickness, materials properties or coating are intentionally produced [2]. The first TWB applications were implemented on the automotive sector as welding stage prior to forming, aiming at optimization and better control of material flow and usage during forming [2,3]. However, welding high performance lightweight alloy, especially in dissimilar configuration (different thickness or materials), is a rather complex task to be achieved by conventional fusion-based welding technologies mainly due to the sensitivity to defect formation, such as solidification cracking. Therefore, alternative solid-state based welding technologies have been successively applied to produce tailor-welded blanks joints mainly produced with thin high-performance aluminum sheets focused on automotive applications [4–8].

In this context, there is a need for development and assessment of thicker TWBs designed for the shipbuilding sector [9]. Therefore, this paper explores the mechanical performance and microstructural features of dissimilar friction stir welded TWBs produced with alloys of particular interest to the shipbuilding sector (AA6082 and AA5083) and thicker plates. Moreover, it attempts to show the effect of rotational speed on the weld properties, such as presence of a remnant oxide line at the stir zone and its influence on joints local and global mechanical performance.

Experimental procedure

TWBs were produced with extruded AA6082-T6 (6 mm thickness) and cold rolled AA5083-H11 (8mm thickness) plates measuring 200mm x 500 mm. The dissimilar materials were welded by FSW in a single run and the thicker material was placed on the advancing side (AS) of the joint in order to facilitate its complete volume plasticization and mixing. This approach is preferable since FSW generates an asymmetric temperature profile and expose the advancing side to higher temperature and strain rates during welding [9,10]. Fig. 1 presents a schematic view of the welding approach and the geometry of the welding tool used to produce the TWBs. The difference in thickness was compensated by a side tilt angle of 5.7° towards the thinner plate as previously reported [9,11,12]. Four sets of different process parameters were used to induce changes on heat inputs (HI) and therefore, evaluate the effect of rotational speed on the joint properties. Table 1 presents the process parameters, the torque measured by the welding system, power and heat input, which was calculated similarly to that reported by Cui [13].

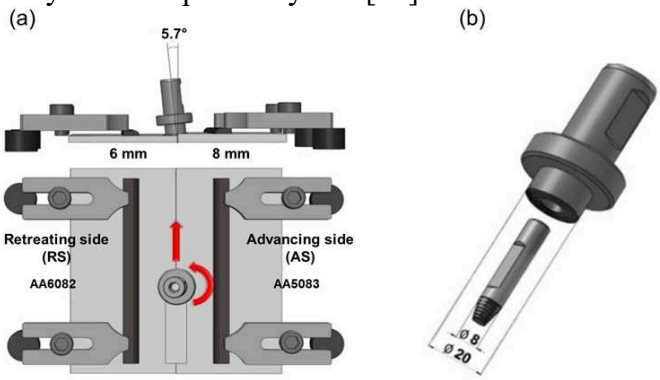

Figure 1: Welding approach (a) and tool geometry (b). The FSW tool consists of a threaded conical pin, with three flats and a spiral (scroll) shoulder with a diameter of 20mm.

Table 1: Process parameters

Joints	RSp [rpm]	WSp [mm/s]	ZF [N]	Torque [Nm]	Q [W]	HI (J/mm)
TWB-1	600	6	20	56.87	3577.24	596.21
TWB-2	600	6	15	52.76	3318.71	553.12
TWB-3	800	6	15	44.54	3735.54	622.59
TWB-4	1000	6	15	38.99	4087.58	681.26

Where: RSp - rotational speed, WSp – welding speed, ZF – Axial force, Q – power and H.I – heat input

The produced TWB joints were examined by optical microscopy and for that welded samples were mounted, ground, and polished up to 0.05µm colloidal silica suspension. The microstructural features were revealed by electrochemical etching using Baker's reagent and polarized light was applied to obtain color contrast of the materials microstructure. The fracture surfaces of the mechanically tested specimens were assessed by scanning electron microscopy using a Quanta^{TM} 650 FEG microscope. The thermal-induced effect of the FSW process on the local mechanical properties across the welded TWB joint was determined by microhardness testing, according to ASTM E384 standard and using a Zwick/Roell ZHV microhardness machine. Indentations spaced in 0.5 between each other were carried out on the center of the cross-section samples using a load of 0.2 kgf applied for 10 seconds. The quasi-static performances of the joints were assessed trough tensile tests using a Zwick/Roell universal testing machine according to the ASTM E8M. Three specimens were tested at room temperature for all joint configurations. The test was carried out in a constant crosshead speed of 1 mm/min and a digital image correlation system (DIC), from GOM, was linked to the tensile test machine and used to assess the local strain behavior of the joints during the test. The obtained data was evaluated with the integrated software ARAMIS.

Results and discussion

During the whole FSW process, spindle torque was monitored by the welding system and the average values for each welding condition are presented in the Fig. 2, as well as the calculated HI. Torque and HI displayed a hyperbolic curve according to the increase on rotational speed (RSp). Moreover, the RSp increase caused an opposite effect on these parameters. While the torque decreased with increasing RSp the HI increase. This is caused by the increase in plastic deformation and temperature induced by higher RSp. Higher rotational speeds lead to higher temperatures in the stirred zone and as result more plasticized material is formed around the FSW tool. Consequently, lower torque is required from the welding system to rotate the tool and produce the welded joint.

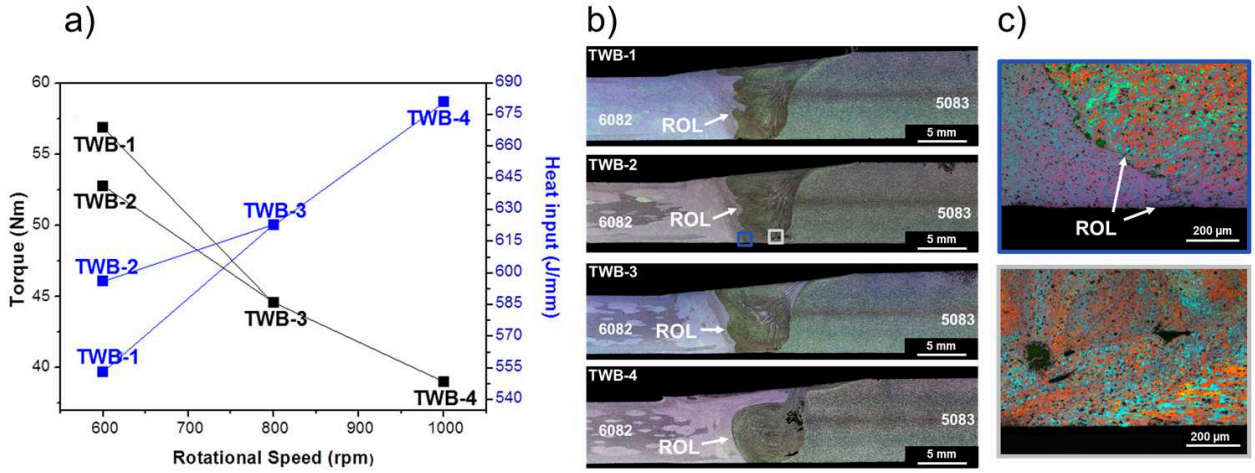

Figure 2: Effect of process parameters on torque and heat input for all weld experiments (a), cross-sectional view of the TWB welds (b), and details of the ROL and defect at SZ (c).

Apart from the processing point of view, the increase in RSp severely changes the microstructural features of the TWBs base materials, particularly at the central portion of the joints. Microstructure analysis revealed the presence of a remnant oxide line (ROL) at the stirred zone (SZ) for all welding conditions (Fig. 2 (b) and (c)). The ROL formation is related with two factors: the original oxide layer presented on the base materials surface and, the agglomeration of inclusion particles (oxides) at the materials interface, which are present in large quantities in the AA6082. Moreover, the rotational speed directly affected the ROL distribution, as shown in Fig. 2(b). Low rotational speeds (600 rpm – TWB-1 and 2) induce the formation of a zig-zag shape of the ROL while higher rotational speeds (for instance 1000 rpm – TWB-4) tend to produce an onion-ring appearance. Defect formation at the advancing side of the joints were also observed for all welding conditions (Fig. 2 (b) and detail at Fig. 2 (c)), which may be related to insufficient axial force during the welding process, and difficult to plasticize and mixing of the dissimilar materials. Further process parameters optimizations are still required in order to produce defect-free joints.

The process induced changes on microstructure were similar to all welding condition investigated in this work; therefore condition TWB-1 was selected to present a typical microstructural features of the produced TWBs joints, Fig 3. As have been reported in the literature for similar FSW processes [9,14], the microstructure of the central portion of the joints, SZ, has been dynamically recrystallized and present a fine-grained, equiaxed microstructure, Fig. 3(c). Adjacent to the SZ, a thermo-mechanically affected zone (TMAZ) was formed on both welding sides (AS and RS) and highly deformed grains resulting from the material flow were observed, Fig. 3(d). In Fig. 3(e) a detailed view of the ROL is presented. As the base materials respond differently to the chemical etchant used to reveal the microstructure, it is possible to precisely identify the distribution of the ROL and the interface between both materials. Fig. 3 (f) depicted the tunnel defect on the joints AS previously mentioned, which has acceptable dimension according to ISO 25239-5.

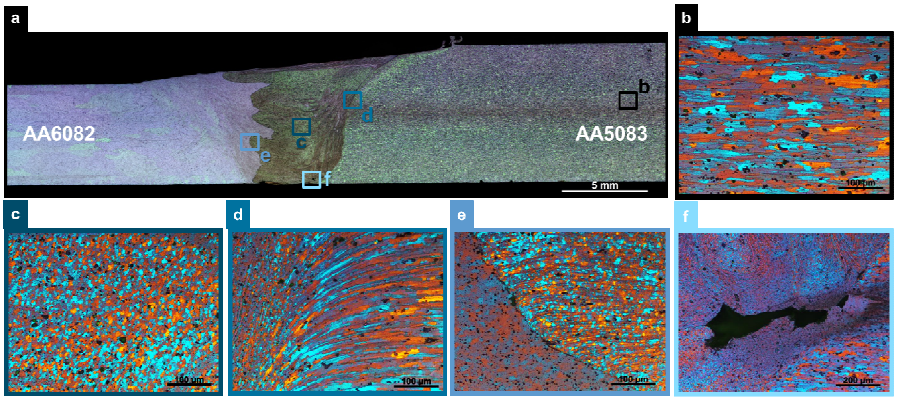

Figure 3: Microstructural features of a typical TWB weld by FSW: (a) cross-sectional view of the weld, (b) the AA5083 base material microstructure, (c) stirred zone, (d) the thermo-mechanical affected zone, (e) remnant oxide line (ROL) and (f) tunnel defect at the AS.

The thermo-mechanically-induced process changed locally the mechanical properties of the joints, especially on the RS of the TWBs, where the heat-treatable aluminum alloy was placed (AA6082). The temperatures reached during the welding process were probably high enough to dissolve the precipitates presented on the AA6082 base materials. Therefore, a reduction of microhardness was observed (from 115 HV down to 68 HV), Fig. 4(a). As the hardness mechanism of the AA5083 base materials is not sensitive to the process temperature, its microhardness does not vary throughout the indentation line. Moreover, the increase on HI tends to increase the size and dislocate the heat-affected zone further away from the SZ, Fig. 4 (b).

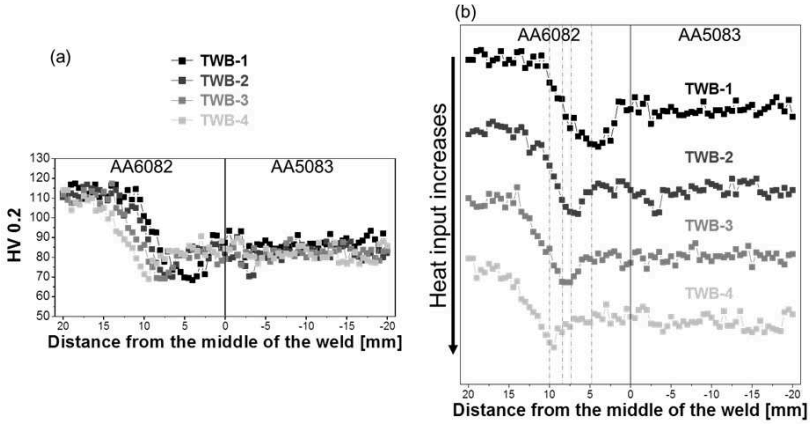

Figure 4: Vickers microhardness profile of all TWB joints (a) and effect of the heat input on the microhardness profile of the TWBs (b).

Fig. 5 presents the global mechanical performance of the TWBs under quasi-static loading. The increasing in RSp systematically decreases the mechanical performance of the TWBs. It is believed that the distribution of the ROL plays a significantly contribution in this behavior. The distribution in a zig-zag shape tends to retard the crack propagation, while an onion-ring shape displays an easy path for cracks propagation. The TWBs produced with low rotation speeds and axial force of 20 kN have shown higher mechanical performance, as observed on Fig. 5(c) and failed at the TMAZ of the AA6082 plate (Fig 5(b)). Two different types of failure were observed during the mechanical test. The first correspond to a fracture located at the TMAZ of the RS (AA6082) of TWBs, as previously mentioned, and it was observed for the condition TWB-1. This joint sustained more loading and plastic deformation as shown in the strain maps of Fig. 5(b). The other conditions result in fracture trough the stirred zone and the failure propagates following the ROL (Fig. 6). However, in both cases the strain concentration at the beginning of the test is located on the TMAZ at the RS, as shown on the strain maps obtained by DIC. This behavior is caused by the local changes on mechanical performance of the AA6082 TMAZ as discussed on the microhardness profiles and the stress concentration factor induced by the difference in thickness.

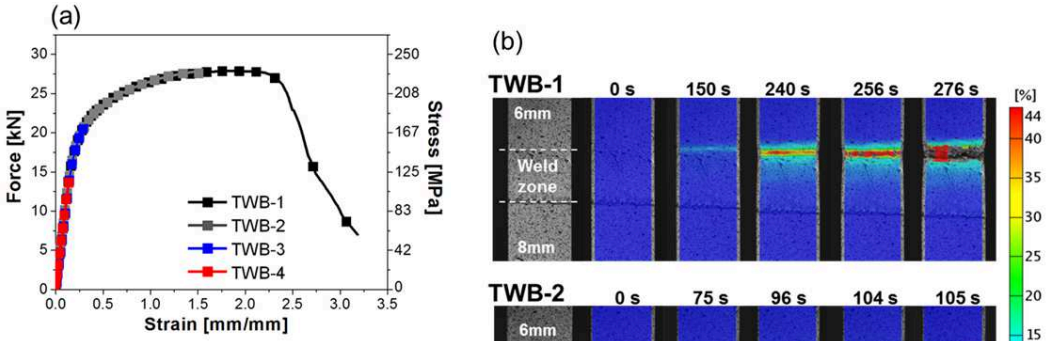

(c)

Specimen name	Av. $Rp_{0.2}$ [N/mm²]	Av. R_m [N/mm²]	Av. A [%]
TWB-1	125.5 ± 0.6	154.4 ± 1.5	3.1 ± 0.1
TWB-2	126.3 ± 0.2	148.0 ± 6.1	1.1 ± 0.4
TWB-3	117.7 ± 5.5	**	0.3 ± 0.1
TWB-4	104.6 ± 25.9	**	0.4 ± 0.3

** brittle fracture

Figure 5: Tensile stress-strain curve for the TWB joints (a), mechanical properties of the joints (B) and strain maps obtained by DIC.

The fracture surface analyses of the tested TWBs revealed that the welding condition TWB-1 underwent considerable plastic deformation prior to the fracture. As a result, a variety of dimples with different sizes were observed on the fracture surface. For the other welding conditions, in which the fracture took place at the SZ, flow marks were exposed. These marks are created by each revolution of the FSW tool during the welding. As the RSp increase, the number of revolution per millimeter carried out by the tool increase (higher weld pitch), and these marks systematically tend to come near to each other. Thus, a smooth fracture surface is formed (see the difference between TWB 2, 3 and 4). The onion-ring shape of the ROL (TWB-4) resulted in a brittle fracture and its fracture surface displayed a smooth surface with almost no observed plastic deformation.

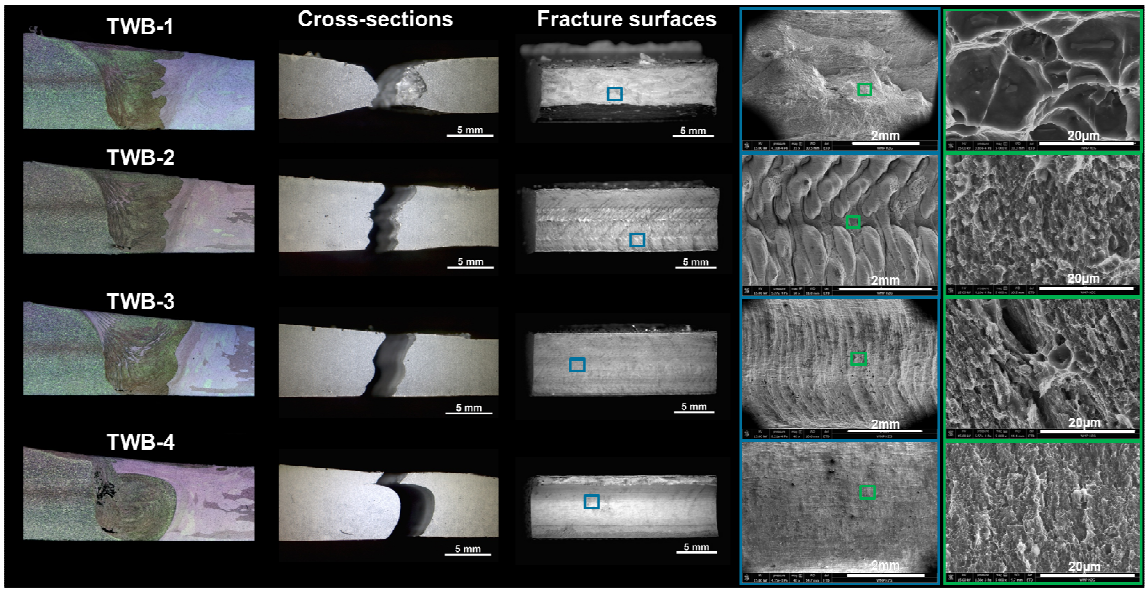

Figure 6: SEM fracture surface of the TWBs.

Conclusions

In the present study, TWBs were produced with dissimilar materials (AA6082 and 5083) and thickness (6 and 8 mm). The results revealed the presence of ROL at the stirred zone (formed by the agglomeration of inclusion particles and oxides), and describe the effect of rotational speed on its distribution and influence on the mechanical properties of the welds. The TWBs produced with low RSp (600 rpm) showed higher mechanical performance and failed at the TMAZ of the AA6082. However, by increasing the RSp up to 1000 rpm an onion-ring distribution of the ROL was

achieved and, as a result, the mechanical performance was considerable affected. The tunnel defect present on the AS presented acceptable dimension according to ISO 25239-5 and therefore, it does not influence the fracture mechanisms of the TWB, since the joints failure either at the TMAZ or through the ROL.

Acknowledgments

The authors would like to acknowledge the financial support provided to E. E. Feistauer by the *Conselho Nacional de Pesquisa* - CNPq (Brazil).

References

[1] S. Ferraris, L.M. Volpone, Aluminium alloys in third millennium shipbuilding: materials, technologies, perspectives, in: Fifth Int. Forum Alum. Ships Tokyo Jpn., 2005.
[2] M. Merklein, M. Johannes, M. Lechner, A. Kuppert, A review on tailored blanks—Production, applications and evaluation, J. Mater. Process. Technol. 214 (2014) 151–164.
[3] B.L. Kinsey, 7 - Tailor welded blanks for the automotive industry, in: Tailor Welded Blanks Adv. Manuf., Woodhead Publishing, 2011: pp. 164–180.
[4] A.A. Zadpoor, J. Sinke, R. Benedictus, R. Pieters, Mechanical properties and microstructure of friction stir welded tailor-made blanks, Mater. Sci. Eng. A. 494 (2008) 281–290.
[5] A.A. Zadpoor, J. Sinke, R. Benedictus, Global and Local Mechanical Properties and Microstructure of Friction Stir Welds with Dissimilar Materials and/or Thicknesses, Metall. Mater. Trans. A. 41 (2010) 3365–3378.
[6] C. Leitão, B. Emílio, B.M. Chaparro, D.M. Rodrigues, Formability of similar and dissimilar friction stir welded AA 5182-H111 and AA 6016-T4 tailored blanks, Mater. Des. 30 (2009) 3235–3242.
[7] K. Chung, W. Lee, D. Kim, J. Kim, K.-H. Chung, C. Kim, et al., Macro-performance evaluation of friction stir welded automotive tailor-welded blank sheets: Part I – Material properties, Int. J. Solids Struct. 47 (2010) 1048–1062.
[8] M. Garware, G.T. Kridli, P.K. Mallick, Tensile and Fatigue Behavior of Friction-Stir Welded Tailor-Welded Blank of Aluminum Alloy 5754, J. Mater. Eng. Perform. 19 (2010) 1161–1171.
[9] E.E. Feistauer, L.A. Bergmann, L.S. Barreto, J.F. dos Santos, Mechanical behaviour of dissimilar friction stir welded tailor welded blanks in Al–Mg alloys for Marine applications, Mater. Des. 59 (2014) 323–332.
[10] R. Nandan, T. DebRoy, H.K.D.H. Bhadeshia, Recent advances in friction-stir welding – Process, weldment structure and properties, Prog. Mater. Sci. 53 (2008) 980–1023.
[11] A. von Strombeck, S. Sheikhi, J.F. dos Santos, Effect of Welding Speed on the Properties of Friction Stir Welded Tailored Blanks, in: 4th Int. Symp. Frict. Stir Weld., Park City, Utah, USA, 2003.
[12] S. Sheikhi, J.F. dos Santos, On the Formability of Friction Stir Welded Aluminium Tailored Welded Blanks, in: Proc. Int. Symp. Frict. Stir Weld., 2004.
[13] S. Cui, Z.W. Chen, J.D. Robson, A model relating tool torque and its associated power and specific energy to rotation and forward speeds during friction stir welding/processing, Int. J. Mach. Tools Manuf. 50 (2010) 1023–1030.
[14] N. Huber, J. Heerens, On the effect of a general residual stress state on indentation and hardness testing, Acta Mater. 56 (12) 6205–6213.